



Constraining sub-structures in TeV-emitting gamma-ray blazars with the GMVA

J. Heßdörfer^{1,2}, L. Ricci^{1,2}, M. Kadler¹, P. Benke², D. Dorner¹, F. Eppel^{1,2}, C. M. Fromm¹, M. Giroletti³, S. Koyama^{4,5}, A. Kraus², T. P. Krichbaum², R. Lico^{3,6}, K. Mannheim¹, R. Ojha⁷, E. Ros², F. Rösch^{1,2}, and J. Sitarek⁸

¹ Julius-Maximilians-Universität Würzburg, Institut für Theoretische Physik und Astrophysik, Lehrstuhl für Astronomie, Emil-Fischer-Straße 31, D-97074 Würzburg, Germany

² Max-Planck-Institut für Radioastronomie, Auf dem Hügel 69, D-53121 Bonn, Germany

³ INAF – Istituto di Radioastronomia, Via Gobetti 101, I-40129 Bologna, Italy

⁴ Graduate School of Science and Technology, Niigata University, 8050 Ikarashi 2-no-cho, Nishi-ku, Niigata 950-2181, Japan

⁵ Institute of Astronomy and Astrophysics, Academia Sinica, 11F of Astronomy-Mathematics Building, AS/NTU No. 1, Sec. 4, Roosevelt Rd, Taipei 10617, Taiwan, ROC

⁶ Instituto de Astrofísica de Andalucía-CSIC, Glorieta de la Astronomía s/n, E-18008 Granada, Spain

⁷ National Aeronautics and Space Administration Headquarters, 300 E St SW, Washington, DC 20546-0002, USA

⁸ University of Lodz, Faculty of Physics and Applied Informatics, Department of Astrophysics, 90-236 Lodz, Poland

Abstract. Blazars are found to cover a broad range in luminosity and the lowest-luminosity objects turn out to be the ones whose spectral energy distribution extends to the highest energies. In the most extreme blazars their spectral energy distribution can peak at very high gamma-ray energies above 10 TeV. These extremely high peaked BL Lac objects typically are faint radio sources and thus make up a poorly studied source sample, especially at high radio frequencies. Due to their relatively low redshifts, VLBI observations of such sources can achieve very high linear resolution, which makes it possible to constrain limb brightened and/or spine-sheath structures on the smallest accessible scales with the Global Millimetre VLBI Array (GMVA) at 3 mm. The GMVA imaging capabilities are of particular importance as such jet sub-structures might explain the origin of the seed photons for high-energy processes. Here, we present first results of the (sub-)parsec-scale jet morphology in a sample of GMVA observed extreme blazars.

1. Introduction

Blazars are a subclass of Active Galactic Nuclei (AGN) that have their relativistic jets pointed at a small angle to the line of sight towards Earth and exhibit variable emission across the entire electromagnetic spectrum. Their emission has a characteristic double-humped spectrum with the position of the two emission peaks depending on the jet power (e.g., Fossati et al. 1998, Ghisellini et al. 1998). The class of high-peaked BL Lac objects (HBLs) are canonically defined as the group of objects whose primary emission hump peaks above 10^{15} Hz (Padovani & Giommi 1995). In the most extreme cases, the peaks of HBLs can be shifted by up to two orders of magnitude further up (Biteau et al. 2020) into the TeV γ -ray regime. These extreme blazars form a numerous but low-luminosity population of blazars so that they are observed only at small redshifts as they are typically very faint radio sources. Nevertheless, due to their relative proximity, VLBI studies of extreme blazars can achieve very high linear resolutions. Biteau et al. (2020) divide the extreme behavior of these objects into three classes: i) objects that become extreme during flares with both peaks shifting to higher energies and then reverting back to their original HBL state, ii) objects without a hard TeV spectrum but

a steady, hard synchrotron spectrum up to 10 to 100 keV and iii) objects that consistently present a hard γ -ray spectrum that peaks above several TeV, showing little variation even during changes in flux density, and whose synchrotron spectrum tends to peak in the X-ray band.

So far, eighty-four blazars have been detected at TeV energies, with HBLs representing by far the largest group¹. However, with the upcoming Cherenkov Telescope Array (Acharya et al. 2019), which will become operational in 2025, this number is expected to increase drastically, necessitating multi-wavelength studies of these objects to further deepen our understanding of them.

While the high energy emission of HBLs and extreme blazars is typically highly variable and thus indicative of high Doppler factors, radio observations of these sources usually suggest low to modest jet speeds and therefore low Doppler factors. One possible solution to this “Doppler Crisis” was suggested by Ghisellini et al. (2005), attributing the high-energy and the radio emission to different regions in a stratified jet model. Such spine-sheath structures can manifest themselves as limb brightening of the jets’ brightness distribution and polarization that can be resolved on VLBI scales.

¹ <http://tevcat2.uchicago.edu/>

Most previous observations of extreme blazars with VLBI have been performed at cm-wavelengths (e.g., Piner & Edwards 2004), however, Piner et al. (2010) conducted observations also at 22 GHz and 43 GHz where they found signs of limb-brightening in the total intensity and spine-sheath structures in the polarized emission. In this proceeding, we present first results of Global Millimetre VLBI Array (GMVA) observations of a sample of TeV-emitting gamma-ray blazars.

2. Source Sample, Observations and Data Reduction

We observed a sample of five extreme blazars (see Table 1) in October 2020 (8th through 11th) with the GMVA at 86 GHz interleaved with 43 GHz VLBA-only scans in full-polarization mode. For our observations, the participating antennas for the 86 GHz observations were Effelsberg (EF), Pico Veleta (PV), Yebes (YS), Onsala (ON), Metsähovi (MH), three KVN stations (KT, KU and KY) along with eight VLBA antennas. For the 43 GHz observations, all ten VLBA antennas participated.

Due to their faint nature, our campaign constitutes the first high radio frequency interferometric observations of these sources in a long time or ever. Our goal is to test whether we can detect spine-sheath structures in fainter sources and at higher frequencies where we can probe even smaller physical scales.

We calibrated the data using both AIPS (Greisen 1990), following the standard procedure for VLBI data reduction, and the CASA-based pipeline `rPicard` (Janßen et al. 2019). For the latter, we followed the approach outlined in Appendix A of Kim et al. (2023) for the 3 mm observations while we used the standard “VLBIhi” settings for the 7 mm data. Out of the two data sets we selected the one of higher quality for imaging in `Difmap` (Shepherd 1997). Finally, to derive the calibrated polarization information, we used the CASA-based pipeline `PolSolve` (Martí-Vidal et al. 2021) to correct for the polarization leakage and apply the D-terms for each antenna. We note that we have not yet done any absolute EVPA calibration and thus will not be making any statements about the EVPA or magnetic field direction in these sources.

To calculate the brightness temperatures T_B of the cores, we fit the visibilities with circular Gaussian components using the `Difmap modelfit` command. Based on these results, we calculated the apparent brightness temperature following, e.g., Kadler et al. 2004 as

$$T_B = 1.22 \times 10^{12} (1+z) \left(\frac{S_\nu}{\text{Jy}} \right) \left(\frac{\nu}{\text{GHz}} \right)^{-2} \left(\frac{d}{\text{mas}} \right)^{-2} \text{ K} \quad (1)$$

where z is the redshift, ν the frequency, S_ν the flux density of the core component and d its full-width at half maximum.

3. Preliminary results

3.1. 7mm observations

In Fig. 1 we show 43 GHz total intensity images of the five target sources with their properties given in Table 1. All sources show a faint, core dominated morphology, while four of them also exhibit low surface brightness jets with hints of wide opening angles and limb brightening. Where available, we cross-checked our results with data obtained by Piner et al. (2010) and found a good agreement in the overall source morphologies. For the remaining two sources we consulted archival MOJAVE observations (Lister et al. 2018) and found the large scale jet direction to be consistent with our higher frequency data. However, quasi-simultaneous BEAM-ME observations of the calibrators show that our derived flux densities are too low by a factor of 3 to 5, depending on the observation. We find a similar result when inspecting single-dish TELAMON (Eppel et al. 2024) observations of the target sources that were performed shortly after the GMVA observations. We are currently still investigating these peculiarities and will attempt to fix the scaling problem by carefully checking contemporaneous BEAM-ME observations.

Table 1. Properties of the target sources at 43 GHz

Source	S_{core} [mJy]	T_B [10^{11} K]
1ES 2344+514	47	> 1.96
OT 546	41	> 7.00
1ES 1959+650	41	> 1.55
Mrk 421	74	> 3.31
OT 169	46	> 2.51

Columns 2 and 3 list the flux densities and their associated brightness temperatures of the core components. The flux densities are derived from a preliminary calibration scheme and represent lower limits.

To calculate the brightness temperatures of the core components, we first computed the resolution limit according to Equation 2 of Kovalev et al. (2005) and found that none of the cores are resolved. Therefore, we used the resolution limit as an upper limit for the size of the components and calculated lower limits for T_B that are given in Table 1. All apparent core brightness temperatures are above the equipartition limit of $\sim 5 \times 10^{10}$ K (Readhead 1994). In this publication, we are using a preliminary calibration scheme which is known to underestimate the true flux densities in the source images. The same is thus true for the preliminary values of the brightness temperature. Therefore, our data suggest that at least intermediate amounts of Doppler boosting occur in these sources. This contradicts the prevailing picture of HBLs having relatively low brightness temperatures (e.g., Piner et al. 2010). Nevertheless, such Doppler factors can be reconciled with the high Doppler factors from high-energy observations by means of different emission regions in a

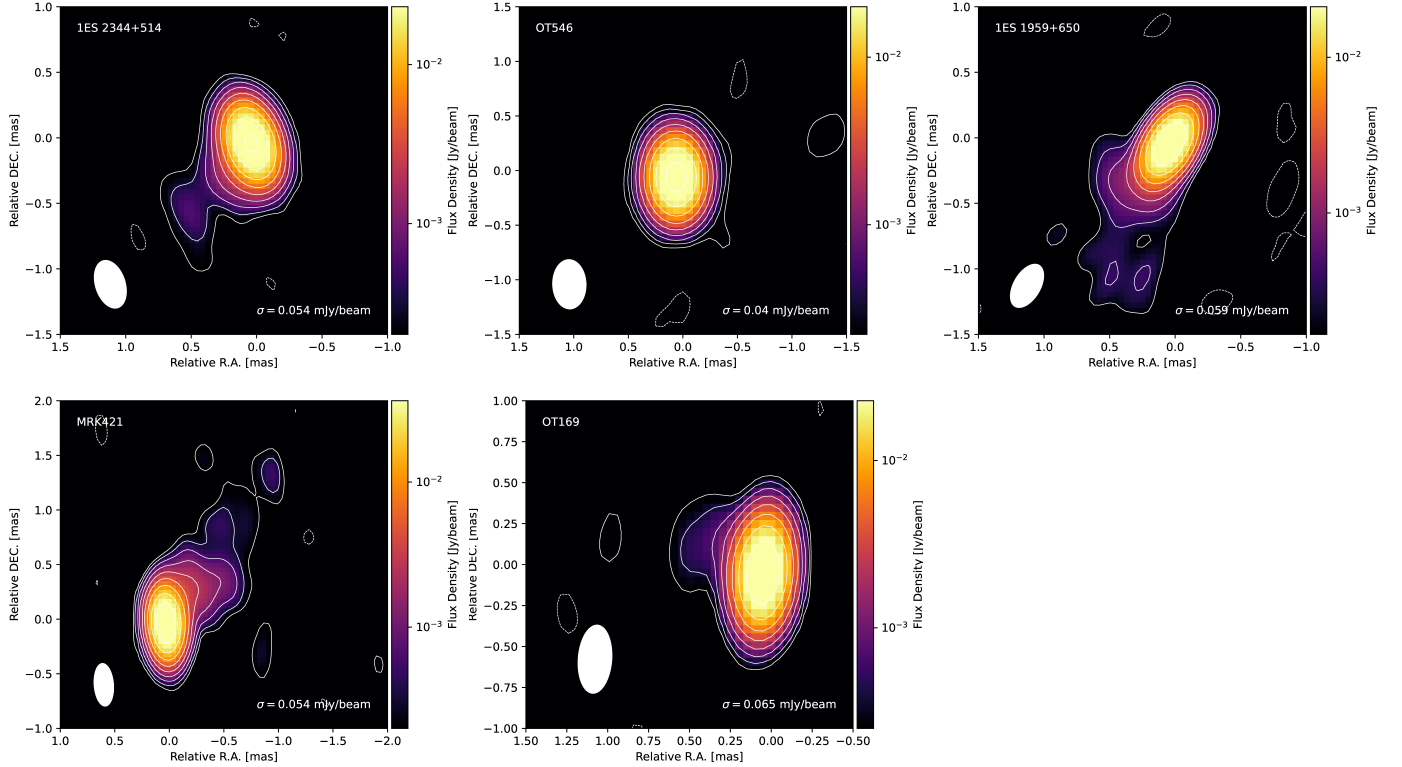


Fig. 1. Total intensity images of the five target sources at 43 GHz (using a preliminary absolute flux-density calibration scheme). The beam is given as the solid ellipse in the bottom left corner. Contours start at 3 times the rms noise given in the bottom right corner and increase logarithmically by factors of 2.

jet that have different Doppler factors, such as the previously mentioned spine-sheath structure. To add onto that, our results might suggest that higher frequency observations probe different regions of the plasma that might be associated with a higher Doppler factor.

Additionally, we imaged the polarized structure of the target sources using PolSolve and successfully detected weak polarized signals in all of them. While the polarization seems to predominantly be present in the core, we also find hints for structures in the jet regions. One example is shown in Fig. 2, where we display the polarized structure of the source Mrk 421 that is in good agreement with previous studies (e.g., Lico et al. 2014, Piner et al. 2010). The fractional polarization in the unresolved core is low ($\sim 3\%$), while the innermost resolved region in the mm-VLBI jet (~ 0.5 mas downstream) shows a considerable fractional polarization of $\sim 20\%$.

3.2. 3mm observations

We are currently working on the calibration of the 3 mm data, which proves to be quite challenging due to the relative faintness of the target sources as well as bad weather conditions during the observations. Nevertheless, in Fig. 3 we show a preliminary 86 GHz image of Mrk 421 that exhibits a well-detected core with a flux density of ~ 100 mJy. As in the case of the 7 mm observations, the preliminary flux-density calibration applied in the reconstruction of

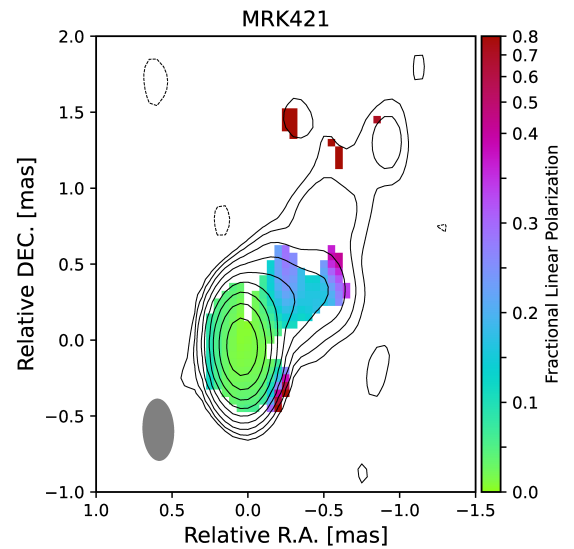


Fig. 2. Fractional polarization of Mrk 421 at 43 GHz plotted on top of the total intensity contours.

the 3 mm brightness distributions underestimates the true flux densities. On top of that, the *modelfit*-component is unresolved, so that we can estimate a lower limit of the core brightness temperature of $T_B > 4.82 \times 10^{11}$ K, again suggesting at least intermediate amounts of Doppler boosting.

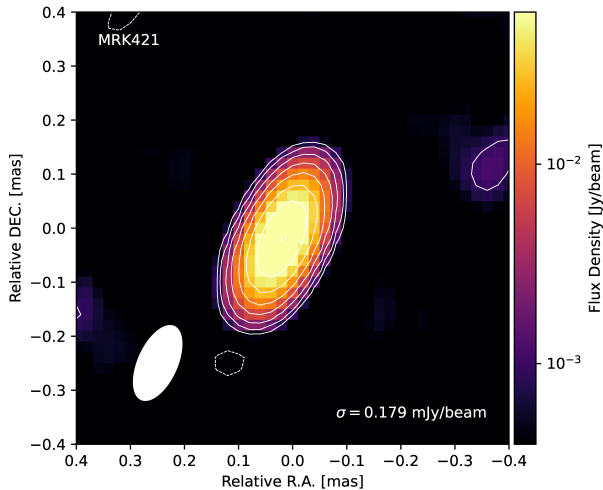


Fig. 3. Total intensity image of Mrk 421 at 86 GHz. The beam is given as the solid ellipse in the bottom left corner. Contours start at 5 times the rms noise given in the bottom right corner and increase logarithmically by factors of 2.

4. Future Prospects

In this proceedings publication, we present first results from a study of a sample of extreme blazars observed with the GMVA in October 2020. Although very challenging due to their low brightness and compact structures, it could be demonstrated that the GMVA can constrain the core brightness temperatures and spatially resolve total and linear polarized brightness distributions at high radio frequencies (7 mm and 3 mm wavelengths). These observables can further constrain physical jet parameters for this important source class such as magnetic field strength and configuration, jet collimation, and structure. Final results of our full set of observational data will be presented in a forthcoming publication. Our goal is to measure intrinsic brightness temperatures of the cores in order to calculate Doppler factors of the jets. To investigate the Doppler Crisis in more detail, we also plan to combine our spatially resolved GMVA data with quasi-simultaneous multiwavelength data that are available to our team and investigate the radio to TeV spectral-energy distributions in the context of multi-zone emission models.

Acknowledgements. This research has made use of data obtained using the Global Millimetre VLBI Array (GMVA), which consists of telescopes operated by the Max-Planck-Institut für Radioastronomie (MPIfR), IRAM, Onsala, Metsähovi Radio Observatory, Yebes, the Korean VLBI Network and the Very Long Baseline Array (VLBA). This research makes use of VLBA data from the VLBA-BU Blazar Monitoring Program (BEAM-ME and VLBA-BU-BLAZAR; <http://www.bu.edu/blazars/BEAM-ME.html>), funded by NASA through the Fermi Guest Investigator Program. FE, FR, MK, LR and JH acknowledge support from the Deutsche Forschungsgemeinschaft (DFG, grants 447572188, 434448349, 443220636, 465409577).

References

- Acharya, B. S., Agudo, I., Al Samarai, I., et al. 2019, *Science with the CTA*. World Scientific, Singapore
- Biteau, J., Prandini, E., Costamante, L., et al. 2020, *Nature Astronomy*, 4, 124
- Eppel, F., Kadler, M., Heßdörfer, J., et al. 2024, *A&A*, 684, A11
- Fossati, G., Maraschi, L., Celotti, A., et al. 1998, *MNRAS*, 299, 433
- Ghisellini, G., Celotti, A., Fossati, G., et al. 1998, *MNRAS*, 301, 451
- Ghisellini, G., Tavecchio, F., & Chiaberge, M. 2005, *A&A*, 432, 401
- Greisen, E. W. 1990, in *Acquisition, Processing and Archiving of Astronomical Images*, 125–142
- Janßen, M., Goddi, C., van Bemmell, I. M., et al. 2019, *A&A*, 626, A75
- Kadler, M., Ros, E., Lobanov, A. P., et al. 2004, *A&A*, 426, 481
- Kim, D.-W., Janssen, M., Krichbaum, T. P., et al. 2023, *A&A*, 680, L3
- Kovalev, Y. Y., Kellermann, K. I., Lister, M. L., et al. 2005, *AJ*, 130, 2473
- Lico, R., Giroletti, M., Orienti, M., et al. 2014, *A&A*, 571, A54
- Lister, M. L., Aller, M. F., Aller, H. D., et al. 2018, *ApJS*, 234, 12
- Martí-Vidal, I., Mus, A., Janssen, M., et al. 2021, *A&A*, 646, A52
- Padovani, P., & Giommi, P. 1995, *ApJ*, 444, 567
- Piner, B. G., & Edwards, P. G. 2004, *ApJ*, 600, 115
- Piner, B. G., Pant, N., & Edwards, P. G. 2010, *ApJ*, 723, 1150
- Readhead, A. C. S. 1994, *ApJ*, 426, 51
- Shepherd, M. C. 1997, in *Astronomical Society of the Pacific Conference Series, Vol. 125, Astronomical Data Analysis Software and Systems VI*, ed. G. Hunt & H. Payne, 77